ESTIMATION OF LONGITUDINAL AND TRANSVERSE IMPEDANCE OF THE SPring-8 STORAGE RING

T. Nakamura
JAERI-RIKEN SPring-8 Project Team
SPring-8, Kamigori-cho, Hyogo JAPAN

abstract

The longitudinal and transverse broad-band impedance of the vacuum chamber of the SPring-8 storage ring was estimated by the numerical simulation.

I. INTRODUCTION

The longitudinal and transverse impedance of the vacuum chamber of the SPring-8 storage ring is estimated with the two-dimensional and three-dimensional simulations by MAFIA[1] T2 and T3, respectively, assuming some models of impedance[2,3,4,5]. The typical cross section of the vacuum chamber is shown in Figure 1 and consists of the beam chamber and the slot-isolated antechamber[6].

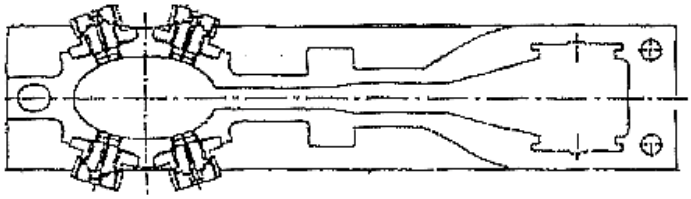

Figure 1. Cross section of the vacuum chamber.

The shapes of the structures of the elements of the beam chamber are shown in Table 1 and Figure 2 and Table 2.

A two-dimensional approximation is used for the elements listed in Table 1. For these elements, the beam pipe is approximated to be a round pipe whose radius is 20mm instead of the real beam pipe shape which is an ellipse whose shorter and longer radii are 20mm and 35mm, respectively. The validity of this approximation is studied in later section.

Table 1. Dimensions of two-dimensional models of elements of the vacuum chamber.

element	dimension [mm, rad]						
	b	b'	d=|b'-b|	g1	g2	θ_1	θ_2
RF cavity	50	250	200	220	220	90	90
weldments	20	22	2	0.2	0.2	90	90
flanges	20	23	3	0.5	0	-	90
offsets	20	20.5	0.5	-	0	0	90
ID section	20	5	15	-	-	5	5
transition at RF section	20	50	30	-	-	10	10
absorbers at RF section	50	35	15	-	-	10	10
BPM	20	-	-	0.5	0.5	90	90

: ID is Insertion Device

: BPM is Beam Position Monitor

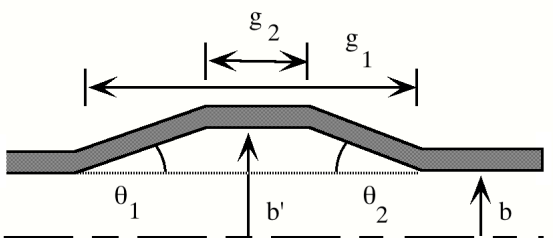

Figure 2. Dimension of two-dimensional models of elements

Table 2. Dimensions of slots

slot	height [mm]	length [mm]	depth [mm]
slot between RF contact fingers	1	1~100	1
slot to antechamber	10 ~ 12	-	> 20
slot to DIP	2	50	4

: DIP is Distributed Ion Pump

II. TRANSVERSE AND LONGITUDINAL WAKE FUNCTIONS

We define (x',y') and q' as the transverse position and the quantity of charge of the driving charge, respectively, and (x_i,y_i) as the transverse position of the axis for integration of wake functions. These are shown in Figure 3.

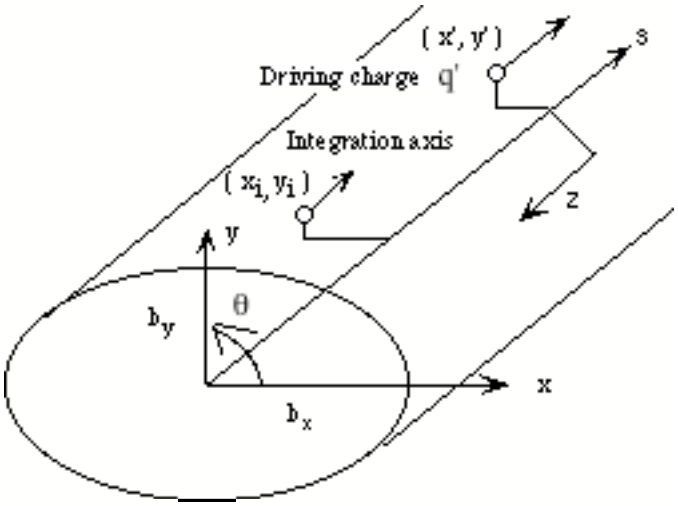

Figure 3. The position (x',y') and charge q' of the driving charge and the position (x_i,y_i) for the integration of wake functions. b_X and b_Y are the pipe radii for x-direction and y-direction, respectively.

1. Impedance of cylindrically symmetric structure

We first summarize the property of the impedance of cylindrically symmetric structure[7].
We set $b_X=b_Y=b$ in Figure 3.

The distribution function $\rho(s,r,\theta)$ of a driving charge at (x',y')=(a,0) is

$$\rho = \frac{q}{a}\delta(s-ct)\delta(r-a)\delta(\theta) \qquad (1)$$

and this can be expressed as a sum of multipole moments;

$$\rho = \sum_{m=0}^{\infty} \rho_m \tag{2}$$

$$\rho_m = \frac{I_m}{\pi\ a^{m+1}(1+\delta_{m,0})}\delta(s-ct)\delta(r-a)\delta(\theta) \tag{3}$$

$$I_m = q\ a^m \quad . \tag{4}$$

We define longitudinal and transverse wake potentials produced by moments $\rho_m(s,r,\theta)$ as

$$\vec{V}_m^{\perp}(z) = \int_{-L/2}^{L/2} ds \quad \vec{F}_m^{\perp} = -eI_m W_m(z) m r^{m-1}\left(\hat{r}\cos m\theta - \hat{\theta}\sin m\theta\right) \tag{5}$$

$$\vec{V}_m^{\parallel}(z) = \int_{-L/2}^{L/2} ds \quad F_m^{\parallel} = -eI_m W_m'(z) r^m \cos m\theta \tag{6}$$

, respectively and corresponding longitudinal and transverse impedance are

$$Z^{\parallel}{}_m(\omega) = \int_{-\infty}^{\infty} \frac{dz}{c} e^{-i\omega z/c} W_m'(z) \tag{9}$$

$$Z^{\perp}{}_m(\omega) = i\int_{-\infty}^{\infty} \frac{dz}{c} e^{-i\omega z/c} W_m(z) \quad . \tag{10}$$

We call $Z^{\parallel}{}_0(\omega)$ longitudinal impedance $Z^{\parallel}(\omega)$ and call $Z^{\perp}{}_1(\omega)$ transverse impedance $Z^{\perp}(\omega)$.

By the Panofsky-Wenzel theorem, $Z^{\parallel}{}_m(\omega)$ and $Z^{\perp}{}_m(\omega)$ have the relation ;

$$Z^{\perp}{}_m(\omega) = \frac{c}{\omega} Z^{\parallel}{}_m(\omega) \quad . \tag{11}$$

On the other hand, with a dimensional analysis, we have a relation between $Z^{\parallel}{}_0(\omega)$ and $Z^{\perp}{}_1(\omega)$;

$$Z^{\perp}{}_1(\omega) \approx \frac{2c}{d^2\omega} Z^{\parallel}{}_0(\omega) \quad \text{or} \quad Z^{\perp}{}_1(\omega) \approx \frac{2c}{d^2\omega_{rev}} \frac{Z^{\parallel}{}_0(\omega)}{n} \tag{12}$$

, where d is a constant of the dimension of length and $\omega = n\omega_{rev}$; ω_{rev} is the angular frequency of revolution. For the resistive-wall impedance and cavity impedance with the diffraction model, this relation is strictly valid if we set d=b. But we have to test the validity of equation (12) for each element.

2. Relation between W_0' / W_1' and $Z^{\parallel}{}_0$ / $Z^{\perp}{}_1$

In the following discussion, we will treat $Z^{\parallel}{}_0(\omega)$, $Z^{\parallel}{}_1(\omega)$ and $Z^{\perp}{}_1(\omega)$. The corresponding wake potentials which are integrated on $(x_i,y_i)=(x,0)$ and are produced by the driving charge whose charge q' is 1C and at (x',y')=(a,0) are

$$V^{\parallel}{}_0(z) = -W_0'(z) \tag{13}$$

$$V^{\parallel}{}_1(z) = -axW_1'(z) \tag{14}$$

$$V^{\perp}{}_1(z) = -aW_1(z) \tag{15}$$

, respectively.

With equation (11) and (12), we can get the relation

$$Z^{\parallel}{}_1(\omega) \approx \frac{2}{d^2} Z^{\parallel}{}_0(\omega) \quad . \tag{16}$$

The corresponding relation between wake functions $W_1'(z)$ and $W_0'(z)$ is

$$W_1'(z) \approx \frac{2}{d^2} W_0'(z) \quad \text{or} \quad b^2 W_1'(z) \approx 2\frac{b^2}{d^2} W_0'(z) \quad \text{or} \quad d^2 W_1'(z) \approx 2W_0'(z) \quad . \tag{17}$$

In terms of the wake potentials (13)-(15), this relation is

$$V^{\parallel}{}_1(z) \approx \frac{2ax}{d^2} V^{\parallel}{}_0(z) \quad . \tag{18}$$

If we set a=x=b, this relation becomes

$$V^{\parallel}{}_1(z) \approx 2\frac{b^2}{d^2} V^{\parallel}{}_0(z) \quad . \tag{19}$$

And if d=b, which is the case of the cavity impedance with the diffraction model or the resistive wall impedance, equation (19) is

$$V^{\parallel}{}_1(z) \approx 2V^{\parallel}{}_0(z) \quad \text{or} \quad b^2 W_1'(z) \approx 2W_0'(z) \quad . \tag{20}$$

Equations (19) or (20) show that, with comparing the shape of $V^{\parallel}{}_0(z)$ and $V^{\parallel}{}_1(z)$, we can test the validity of equation (12) and if equation (12) is valid, we can get a constant d for each element of the vacuum components.

With this scheme, we can test equation (12) intuitively because the function shapes and magnitude of $V^{\parallel}{}_0=-W_0'$ and $V^{\parallel}{}_1=-b^2W_1'$ are almost same. The scheme to compare the shape of W_0' and W_1 is direct but because they have different function shapes, it is more difficult to make comparison.

For three-dimensional structures, W_1 and W_1' are defined for each transverse direction x and y. We call them W_{1x}, W_{1x}' and W_{1y}, W_{1y}', respectively. We assume that the relation (12) is good approximation even in three-dimensional structure.

III. MODEL WAKE FUNCTIONS

With numerical simulations, we can easily obtain the shape of wake potentials, loss parameter kl and the maximum and minimum of wake functions $W^{\parallel}$min, $W^{\parallel}$max or wake potentials $V^{\parallel}$min, $V^{\parallel}$max.

Assuming the models of impedance such as inductive, cavitylike and resistive, we can relate these values; kl, $W^{\parallel}$min and $W^{\parallel}$max to impedance as shown in Table 2[2,3,4]. The shapes of wake functions for those models are shown in Figure 4. We can attach a model to each components of the vacuum chamber by the shapes of their wake functions.

A cavitylike element is a groove with large gap and depth compared with the wave length of interest. The impedance of a shallow groove of which depth is smaller than the wave length of interest is inductive. A shallow cavity or a tapered section is inductive. The simulation with MAFIA T2 shows that a deep groove with small gap compared with the wave length of interest has resistive impedance.

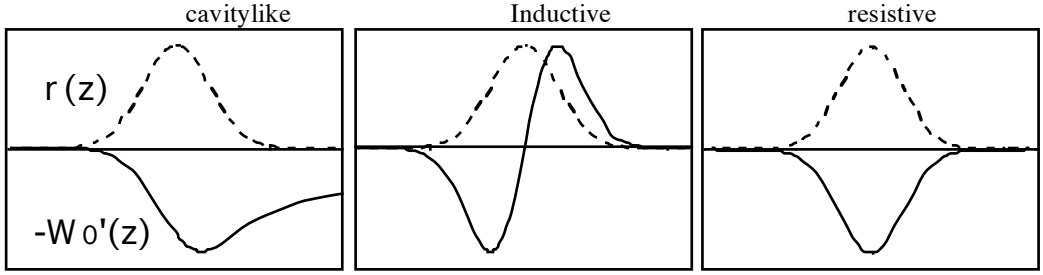

<---------- beam propagating direction ----------

Figure 4. Longitudinal wake functions for cavitylike, inductive and resistive elements.
solid line : Longitudinal wake potential $V^{\parallel}{}_0=-W_0'(z)$
dashed line : Charge density of bunch (Gaussian) $\rho(z)$

Table 3. Longitudinal impedance and $W^{\parallel}_{max}$, kl [2,3,4]

Model	Longitudinal impedance $Z^{\parallel}$		
	Frequency dependence	With $W^{\parallel}_{max}$	With kl
cavitylike	$Z_c \frac{1+i}{\sqrt{\omega}}$	$\frac{1}{1.2824}\frac{\pi}{2}\sqrt{\frac{\sigma}{c}}W^{\parallel}_{max}\frac{1+i}{\sqrt{\omega}}$	$\frac{1}{\frac{\Gamma(1/4)}{4}\frac{2}{\pi}}\sqrt{\frac{\sigma}{c}}k_l\frac{1+i}{\sqrt{\omega}}$
inductive	$-i\omega L$	$-i\omega\sqrt{2\pi e}\left(\frac{\sigma}{c}\right)^2 W^{\parallel}_{max}$	-
resistive	R	$\sqrt{2\pi}\frac{\sigma}{c}W^{\parallel}_{max}$	$2\sqrt{\pi}\frac{\sigma}{c}k_l$

Table 4. Theoretical longitudinal impedance [2,3,4,7]

Model	Theoretical impedance $Z^{\parallel}$
cavitylike	$\frac{Z_0}{2\pi}\frac{1}{a}\sqrt{\frac{cg}{\pi}}\frac{1+i}{\sqrt{\omega}}$
shallow groove	$-i\omega\frac{Z_0}{2\pi c}\frac{g(b'-b)}{b}$
shallow transitions	$-i\omega\frac{3Z_0}{2\pi c}\frac{b(b'-b)^2}{b^2}\left(\frac{2\theta}{\pi}\right)^{1/2}$
resistive wall	$Z_0\frac{1-i}{2}\frac{\delta}{b},\quad \delta=\sqrt{2/\omega\mu\sigma}$
synchrotron radiation	$\left\|Z^{\parallel}\right\| = 300\frac{b}{c}\|\omega\|$

IV. SIMULATION WITH MAFIA

MAFIA calculates the wake potentials. For cylindrically symmetric structures, MAFIA can calculate the wake potentials for each multipole moment. To run MAFIA, we have to define the transverse position (x',y') and charge q' of a driving charge which cause wake and the transverse position (x_i,y_i) of the axis along which wake potentials are integrated, which is shown in Figure 3.

The simulations show that the impedance of the shape II in Figure 5 have weak dependence on the length L, which means that the interference between the wake of the section A and the wake of the section B is small. Based on this fact, we assume that the interference is also small in the shape I. Hence we used shape II instead of the shape I in the simulations for ID sections and RF absorbers of which real shapes are like a shape I . With the shape II, we can use the indirect method to get the wake potentials with MAFIA T2 and T3.

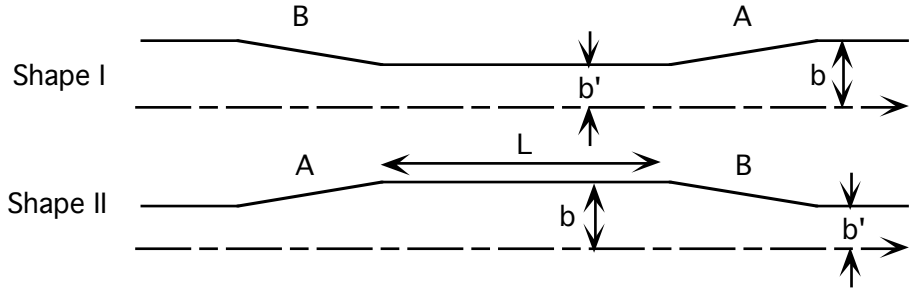

Figure 5. I: real shape, II: shape used in the simulations

V. THE IMPEDANCE OF ELEMENTS

1. wake functions of each element

The wake potentials obtained with MAFIA T2 are shown below for each component of the vacuum chamber. In these simulations, we set q'=1C and $(x',y')=(x_i,y_i)=(\min.\{b,b'\},0)$ hence the obtained wake potentials are $V_{\parallel}^{0}=-W_0'$ and $V^{\parallel}{}_1=-\min.\{b,b'\}^2W_1'$. The impedance obtained with the method mentioned in the section III are shown in Table 4. The d values obtained with the relation (17) or (18) are also shown.

The shapes of Gaussian bunchs which is used in the simulations is shown in Figure 6.

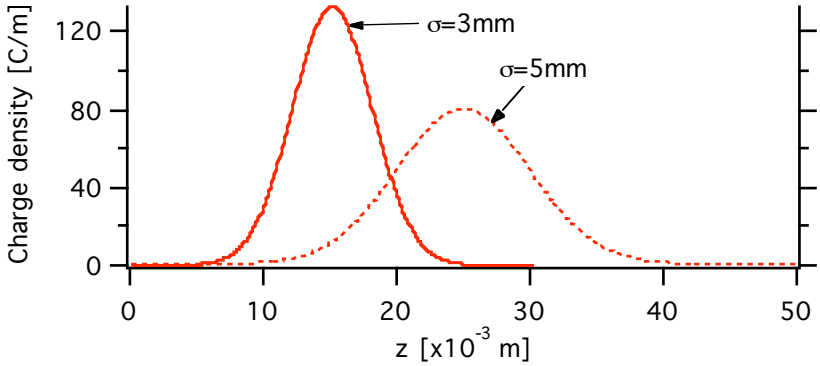

Figure 6. The shapes of bunches for the bunch length is σ_Z = 3mm, 5mm.

The bunch centers are at z=15mm and z=25mm, respectively. The total charge is 1C.

An RF cavity

In the short distance or high frequency region, it has a cavitylike impedance as expected because the ratio of the peak values of $b^2W_1'\text{max}$ / $W_0'\text{max}$ ~ 2. Hence equations (17) or (18) with d=b is good approximation in that region .

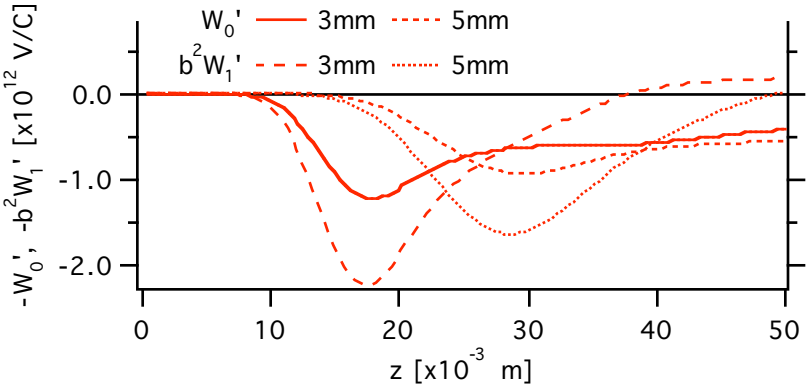

Figure 7. Wake functions of an RF cavity for the bunch length σ_Z = 3mm, 5mm.

The bunch centers are at z=15mm and z=25mm, respectively.

A flange

The gap of a flange is shielded with RF contact fingers. The shape of the residual groove is the triangle shape of the dimension shown in Table 2. The slots are not included in the simulation but the effect of these slots is considered later.

We assume that the theoretical impedance for the small triangular groove is a half of that of the rectangular groove of the same depth and width.

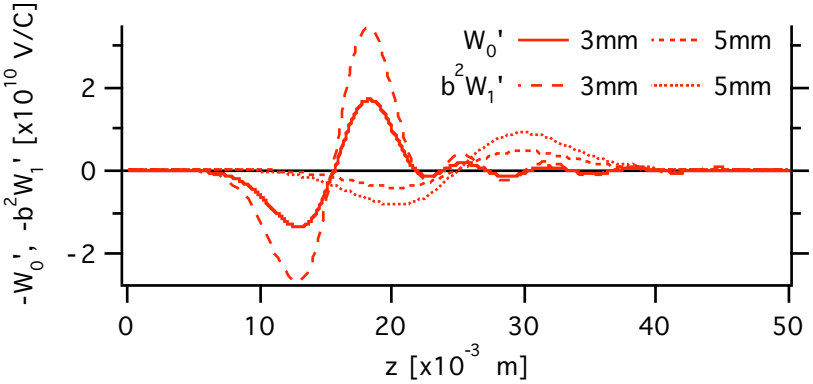

Figure 8. Wake functions of a flange for the bunch length σ_Z = 3mm, 5mm.
The bunch centers are at z=15mm and z=25mm, respectively.

An offset

The residual offsets at the flanges and at the weldments are designed to be less than 0.5mm. The offset is modeled as a step change of the radius.

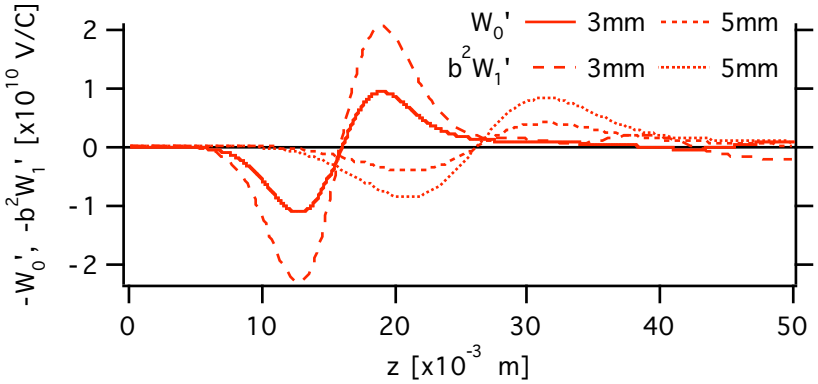

Figure 9. Wake functions of an offset for the bunch length σ_Z = 3mm, 5mm.
The bunch centers at are z=15mm and z=25mm, respectively.

A valve

The shape of the valve is shown in Figure 10. This shape is a set of small structures, such as grooves and small steps. And there are 30 longitudinal slots of (0.5mm wide)×(100mm long) between RF shielding fingers. The wake functions are calculated for each structure and the impedance of the valve is assumed to be the sum of the impedance of them.

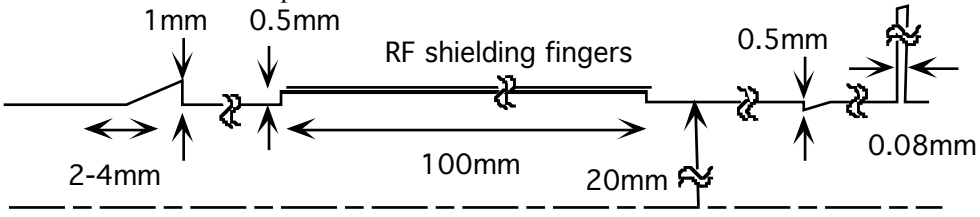

Figure 10. Shape of a valve

Shielded bellows

Bellows are shielded with RF contact fingers and the shape is shown in Figure 11. The impedance is almost inductive.

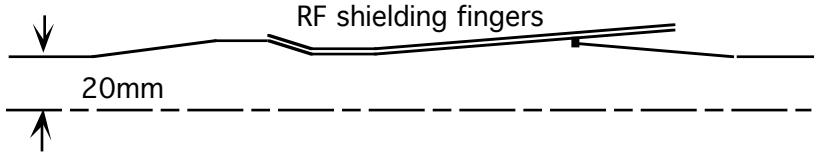

Figure 11. The shape of a bellows.

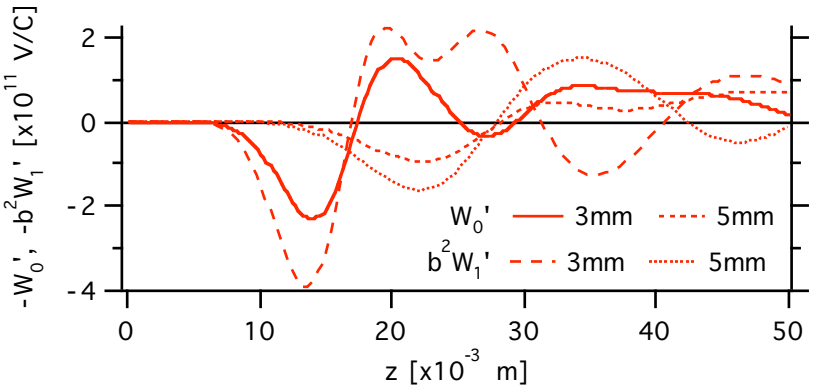

Figure 12. Wake functions of a shielded bellows for the bunch length σ_Z = 3mm, 5mm.
The bunch centers are at z=15mm and z=25mm, respectively.

A beam position monitor

The beam position monitor(BPM) is a button type and consists of four coaxial lines with 0.5mm gap. This structure is modeled with a transverse deep groove of 0.5mm gap. The shapes of the wake functions shown in Figure 13 shows that the impedance is resistive.

The dependence of the impedance of a narrow but deep groove on the gap is shown in Figure 14. This is obtained by the simulation with the bunch length of 3mm, 5mm and 10mm.

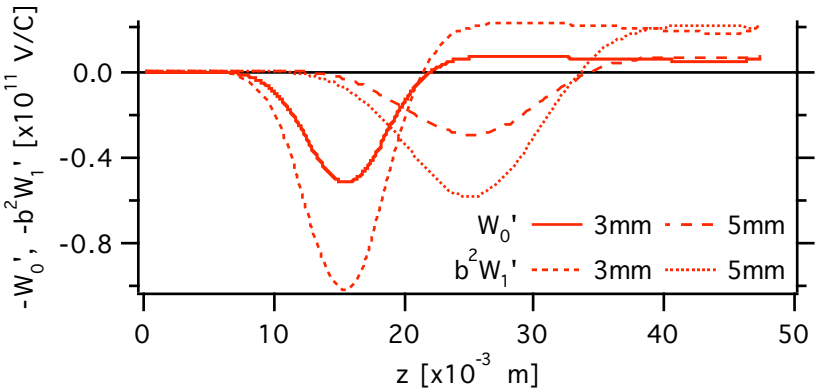

Figure 13. The wake functions of BPM (modeled as a 0.5mm wide transverse slit]
for the bunch length σ_Z = 3mm, 5mm.The bunch centers are at z=15mm and z=25mm, respectively.

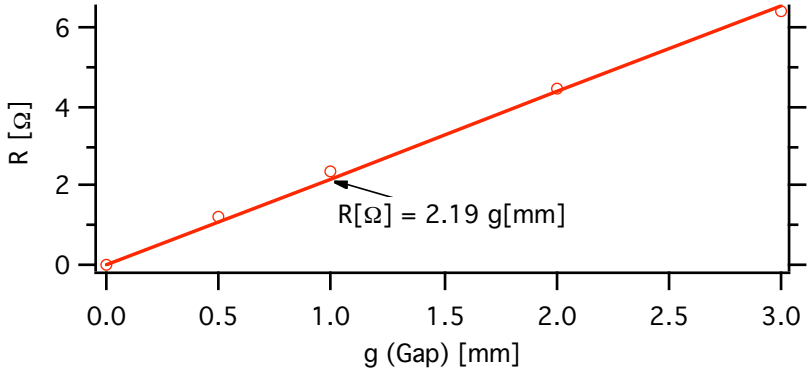

Figure 14. Resistive impedance R of a narrow and deep groove vs. gap g taken by bunch length σ_Z = 3mm, 5mm, 10mm

ID section

The axis of the driving charge and the axis for integration are at (x',y')=(x_i ,y_i)=(b'=gap/2=5mm,0). The results shows that the impedance is inductive and d~10mm. The dependence of the impedance on the taper angle is shown in Figure 16. Also a simulation shows that impedance of an ID section of gap 20mm is half of that of an ID section of gap 10mm and d ~ 15mm.

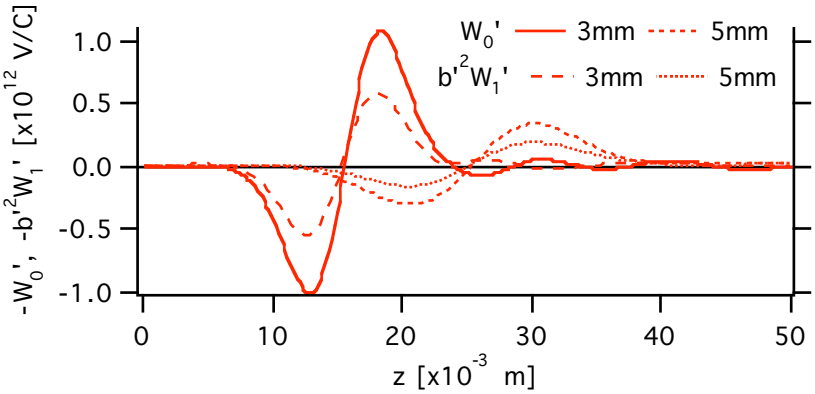

Figure 15. Wake functions of an ID section for the bunch length σ_Z = 3mm, 5mm. The bunch centers are at z=15mm and z=25mm, respectively.

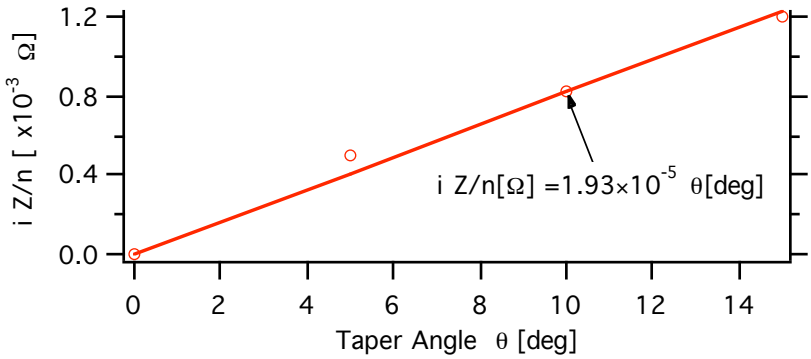

Figure 16. Impedance of the ID sections vs. taper angle θ taken by bunch length σ_Z = 3mm, 5mm, 10mm

Absorbers at RF sections

The shape of the chamber at the absorber at the RF sections is shown in Figure 17. This structure is flexible longitudinally. This shape is approximated as shown in Figure 17.

The impedance is nearly inductive.

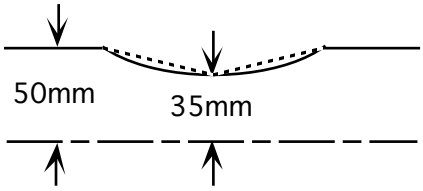

Figure 17. The shape of absorbers at the RF sections(solid line) and the model shape of absorbers at the simulation (dashed line).

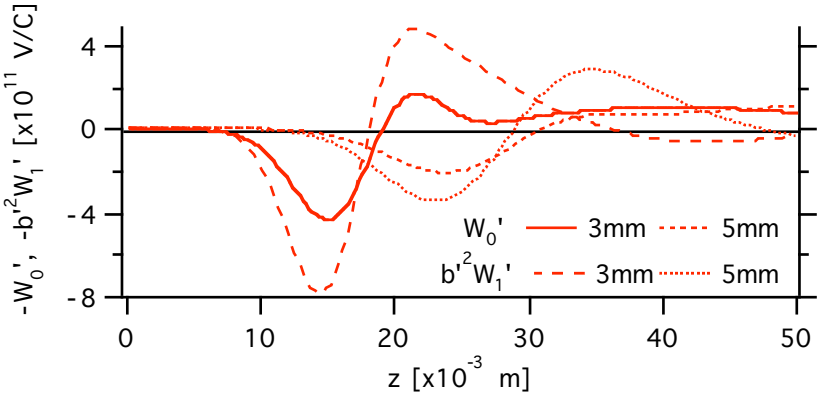

Figure 18. Wake functions of an absorber at RF sections for the bunch length σ_z = 3mm, 5mm. The bunch centers are at z=15mm and z=25mm, respectively.

Transitions at RF sections and normal sections.

The normal section whose pipe radius 20mm and the RF section whose pipe radius 50mm is connected with taper sections of 10 degree gradient. The result shows that d~30mm whereas b=20mm.

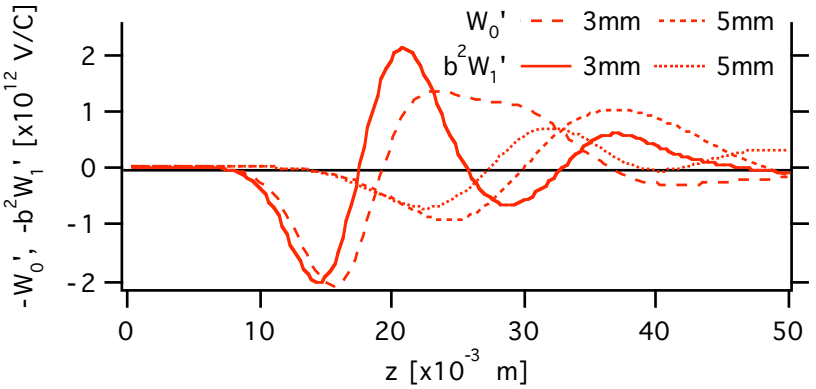

Figure 19. Wake functions of an transition at RF sections slots to antechamber for the bunch length σ_z = 3mm, 5mm. The bunch centers are at z=15mm and z=25mm, respectively.

slots

The slots to antechambers are attached at the position B in Figure 20. The flanges, bellows and valves have RF shielding fingers to shield the large structures such as deep groove or bellows from the beam.

The width of slots between RF shielding fingers is less than 1mm.The effect of slots is estimated in later section.

2. Summary of the impedance

The impedance of each element is Table 5. The wake function of each element also shows that the transverse impedance can be expressed with equation (12). The d values for most elements are the radius of the beam pipe, b. For small angle tapered transitions such as ID sections and transitions at RF sections, d value is more than min.{b,b'}.

Table 5. Impedance of the SPring-8 storage ring

Elements	Number	Total Impedance			d / min.{b,b'} [mm/mm]
		Theory	Simulation		
		$\frac{Z^{\parallel}}{n}$ [Ω]	$\frac{Z^{\parallel}}{n}$ [Ω]	$Z^{\perp}$ [MΩ/m]	
RF cavities	32	$1.5\times10^{5}\frac{1+i}{n\sqrt{n}}$	$1.3\times10^{5}\frac{1+i}{n\sqrt{n}}$	$2.8\times10^{4}\frac{1+i}{n\sqrt{n}}$	50 / 50
weldments	2000	- 0.005 i	- 0.006 i	- 0.007 i	20 / 20
flanges	700	- 0.005 i	- 0.007 i	- 0.008 i	20 / 20
offsets	2700	- 0.013 i	- 0.020 i	- 0.023 i	20 / 20
bellows	400	-	- 0.060 i	- 0.068 i	20 / 20
BPMs	300	-	360 / n	410 / n	20 / 20
transitions at RF sections	4 pair	- 0.007 i	- 0.006 i	- 0.007 i	20 / 20
absorbers at RF sections	8	- 0.007 i	- 0.003 i	- 0.003 i	35 / 35
ID sections	40	- 0.020 i	- 0.020 i	- 0.092 i	10 / 5
valves	100	-	40 / n - 0.003 i	46 / n - 0.003 i	20 / 20
pumping slots	3000	-	-2×10^{-5} i	-2×10^{-5} i	$\left(20/\sqrt{2}\right)/35$
slots to antechamber	500	-	- 0.001 i	- 0.001 i	$\left(20/\sqrt{2}\right)/35$
slots between RF contact fingers	24000	-	- 0.001 i	- 0.001 i	$\left(20/\sqrt{2}\right)/35$
resistive wall (b=20mm)	-	$1.9\frac{1-i}{\sqrt{n}}$	-	$2.2\frac{1-i}{\sqrt{n}}$	20 / 20
synchrotron radiation	-	0.026	-	-	-

: These elements have the RF shielding fingers.

VI. IMPEDANCE OF SLOT

The impedance of slots is estimated with the three-dimensional simulations with MAFIA T3. A model shape is shown in Figure 20. A Slot is attached to the beam pipe vertically (position A) or horizontally (position B). The shape has the two symmetric plane to set boundary conditions. The obtained wake potentials are divided by 2 to get the effect of a single slot. The bunch length used in these simulations is σ_z=10mm and the mesh size is ~1mm.

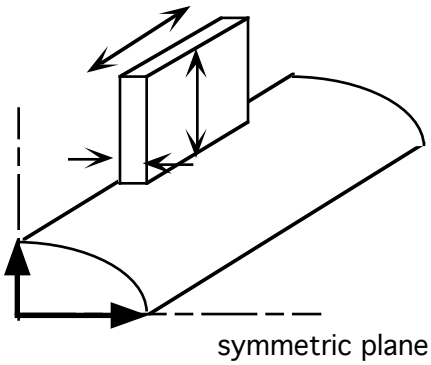

Figure 20. The shape and the slot positions used in the simulations.

The longitudinal functions of slots at the position A and the position B are shown in Figure 21. This shows that the impedance of a slot is inductive. The dependence of the longitudinal impedance on the slot height is shown in Figure 22 for a slot at the position A.

The transverse wake functions for slots at the position A and the position B are shown in Figure 23 and Figure 24, respectively with their longitudinal wake potentials. Because the wake functions obtained with MAFIA T3 is the sum of wake functions of all moments, the transverse offset of the driving charge and the integration axis must be smaller enough than b_x and b_y to get only the effect of dipole moments W_1'. We set them at $(x',y')=(x_i,y_i)=(0,10\text{mm})$ for the slot at the position A and at $(x',y')=(x_i,y_i)=(10\text{mm},0)$ for the slot at the position B. Hence the obtained wake functions are W_0', $(10\text{mm})^2W_{1x}'$, $(10\text{mm})^2W_{1y}'$, $(10\text{mm})\ W_{1x}$ and $(10\text{mm})\ W_{1y}$.

Based on equation (17), $d^2W_1'(z)=2W_0'(z)$, the obtained d value is (by=20mm) /√2 for y direction. which means that the ratio $Z_\perp/Z_{||}$ is 2 times larger than that of cylindrically symmetric structures. If the beam offset is y-direction, the structure at the position B in Figure 20 can produce very small transverse impedance compared to the structure at the position A. But the structure at the position B and at the position A both produce the same amount of the longitudinal impedance. The ratio of the transverse impedance and the longitudinal impedance is almost same in both positions A and B. The reason of the d=(by=20mm) /√2 is supposed to be as follows. The beam pipe is assumed to be round; $b_x=b_y=b$. If the beam pipe has the slots both at both position A and the position B, then the d value should be b. On the other hand, if the beam pipe has the slot only at the position B, the transverse impedance is the same but the longitudinal impedance becomes half hence the d value should be b divided by √2.

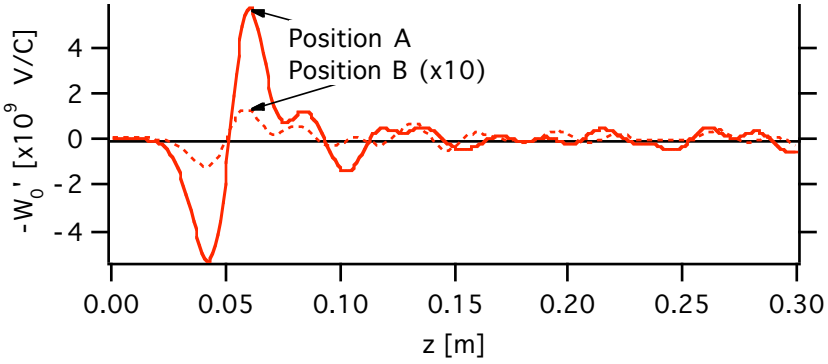

Figure 21. Slot positions and longitudinal wake functions. The slot is (12mm high)×(24mm deep)×(100mm long). The bunch length is σ_Z=10mm and the bunch center is at z=0.05m.

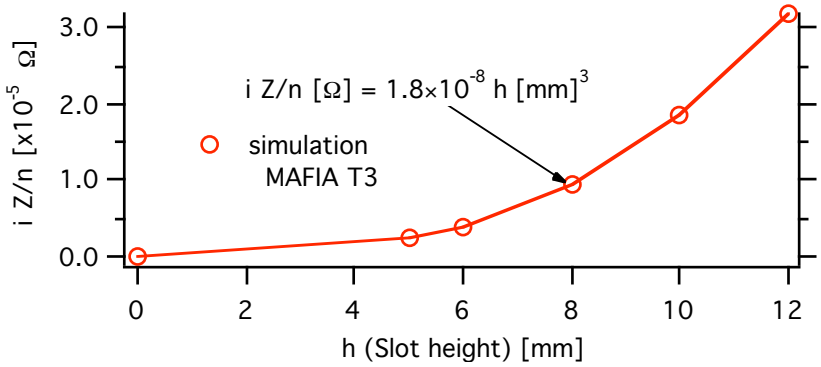

Figure 22. Longitudinal impedance of a slot vs. slot height h. The size of the slot is (100mm long)×(24mm deep). The slot is at the position A. The bunch length is σ_Z=10mm.

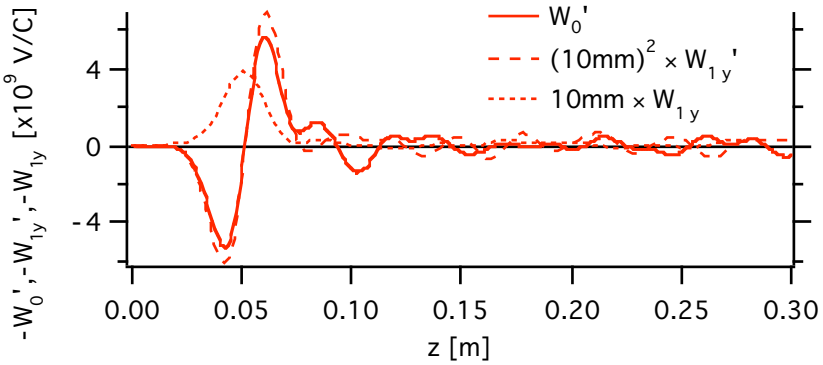

Figure 23. The wake functions for the slot at the position A.
The bunch length is σ_Z=10mm and the bunch center is at z=0.05m.

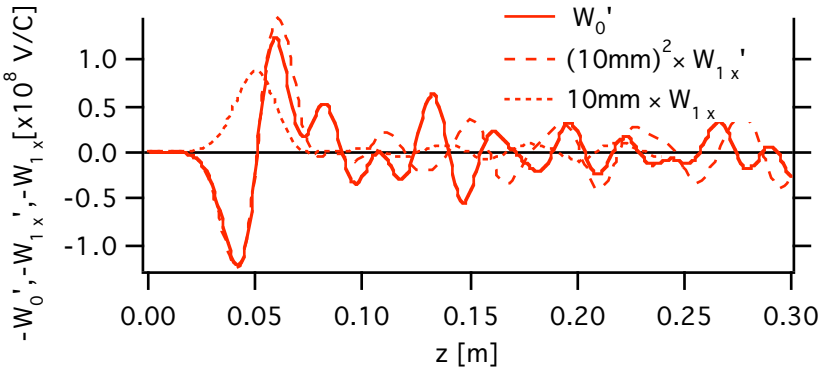

Figure 24. The wake functions for the slot at the position B.
The bunch length is σ_Z=10mm and the bunch center is at z=0.05m.

The effect of the slot shape is estimated for several different types of slots shown in Figure 25. The result is almost same except F as shown in Figure 26-Figure 28. The mesh size is ~1mm.

The simulation shows that the dependence of the impedance of slots on the length and depth of slots are small as shown in Figure 29 and Figure 30. The bunch length is σ_z=10mm.

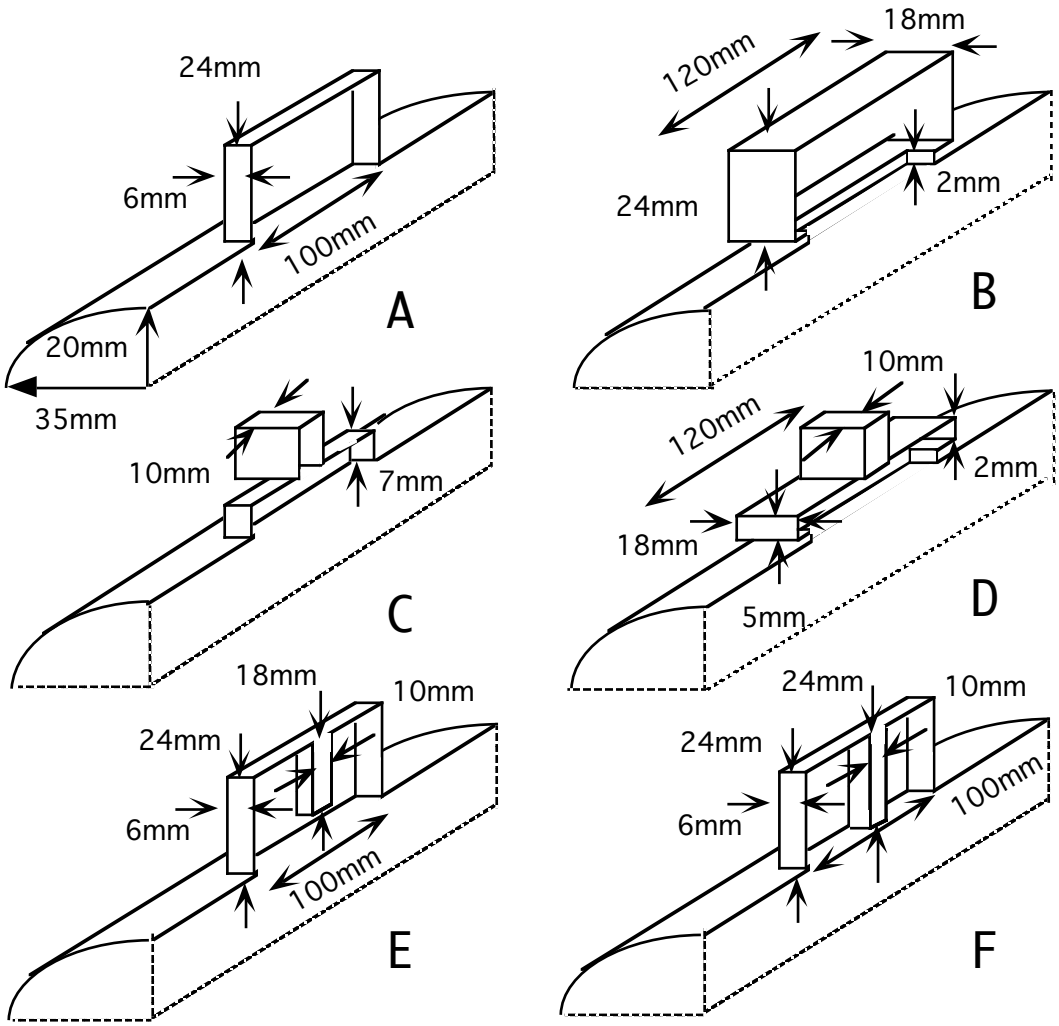

Figure 25. Model slot shapes for the simulation. The slot is (100mm long)×(12mm high)
A,C: slot to antechamber. B,D: slot to D.I.P. E,F: model absorbers in slot.

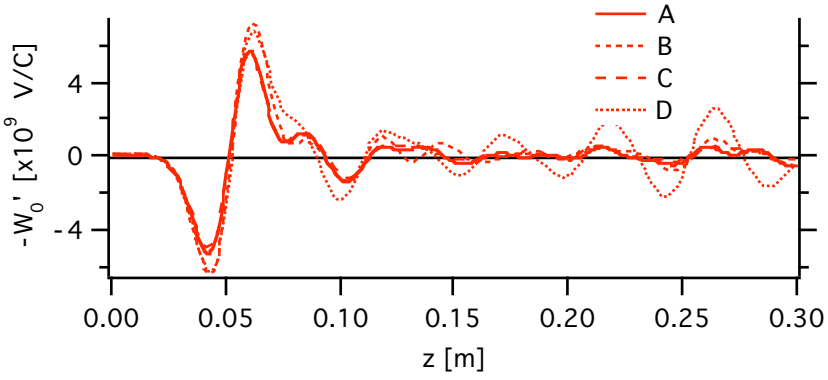

Figure 26. Wake functions for different types of slots; A, B, C, D.
The bunch length is σ_Z=10mm and the bunch center is at z=0.05m.

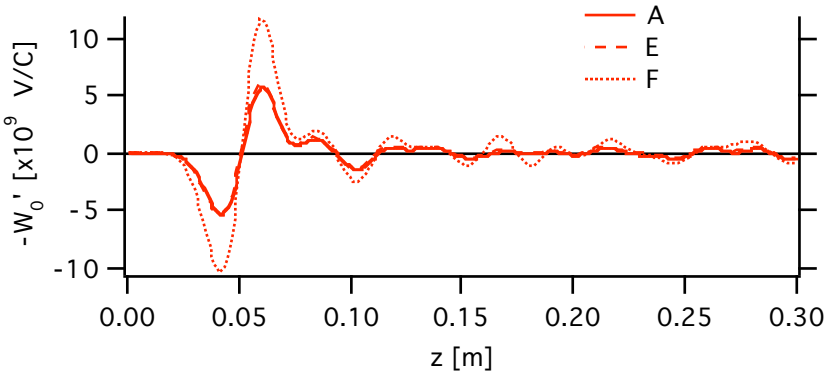

Figure 27. Wake functions for different types of slots; A, E, F.
The bunch length is σ_Z=10mm and the bunch center is at z=0.05m.

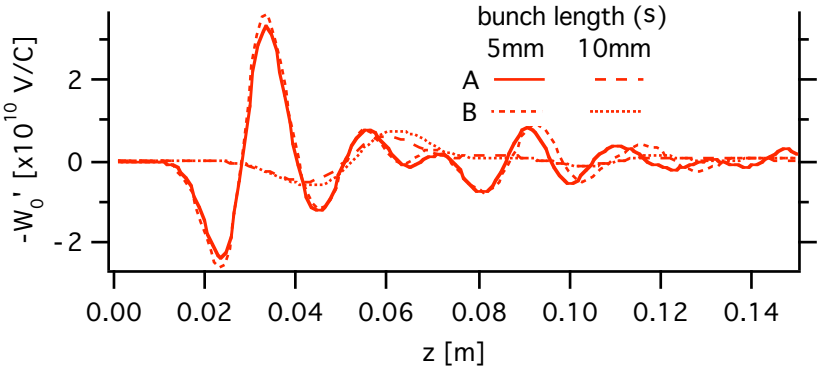

Figure 28. Wake functions for different types of slots; A, B for different bunch length σ_Z=5mm and 10mm. The bunch centers are at z=0.025m and z=0.05m, respectively.

The wake functions of slots of different length and depth are shown in Figure 29 and Figure 30. The impedance of these slots are almost same.

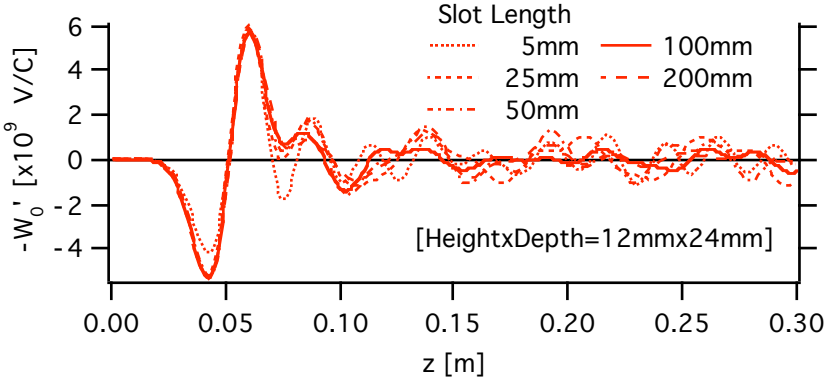

Figure 29. Wake functions of slots of different length.
The bunch length is σ_Z=10mm and the bunch center is at z=0.05m.

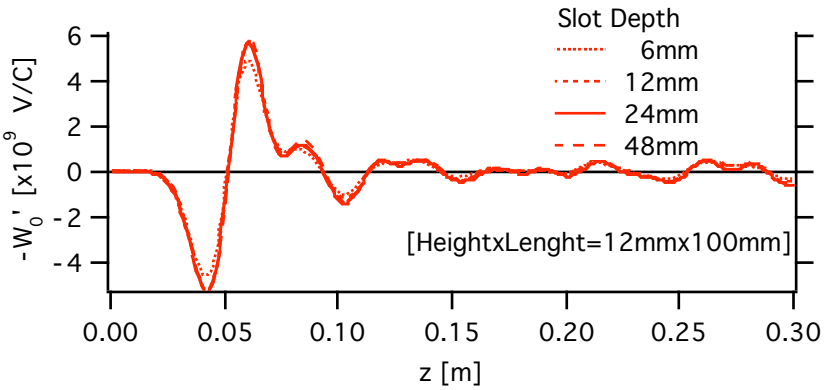

Figure 30. Wake functions of slots of different depth.
The bunch length is σ_Z=10mm and the bunch center is at z=0.05m.

VII. EFFECT OF OBSTACLES IN SLOTS AND ANTECHAMBERS

The effect of obstacles in antechambers is estimated numerically with MAFIA T3 and S3[5]. The structures used in this simulation are shown in Figure 31.

With MAFIA T3, the wake functions are calculated for a test obstacle which is a rectangular hole of (10mm long)×(10mm deep)×(slot height high) opened at the end wall of the slot as shown in Figure 31.

The result for several height of slot(10mm,12mm,14mm) are shown in Figure 32.

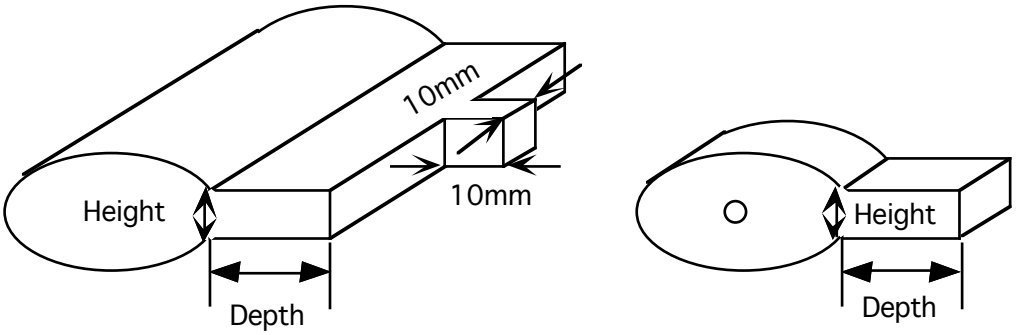

A.: MAFIA T3 B: MAFIA S3

Figure 31. Shapes for the simulation.

The disturbance of the wall current caused by structures generates the wake field hence the strength of the wake field can be estimated from the strength of the wall current flowing at the structure.

With S3, which solves the electrostatic problems, the wall current flowing at the end wall of the slot was calculated. The charge are placed on the beam axis and the induced charge on the end wall of the slot was calculated for several height and depth of the slot. This induced charge is proportional to the wall current.

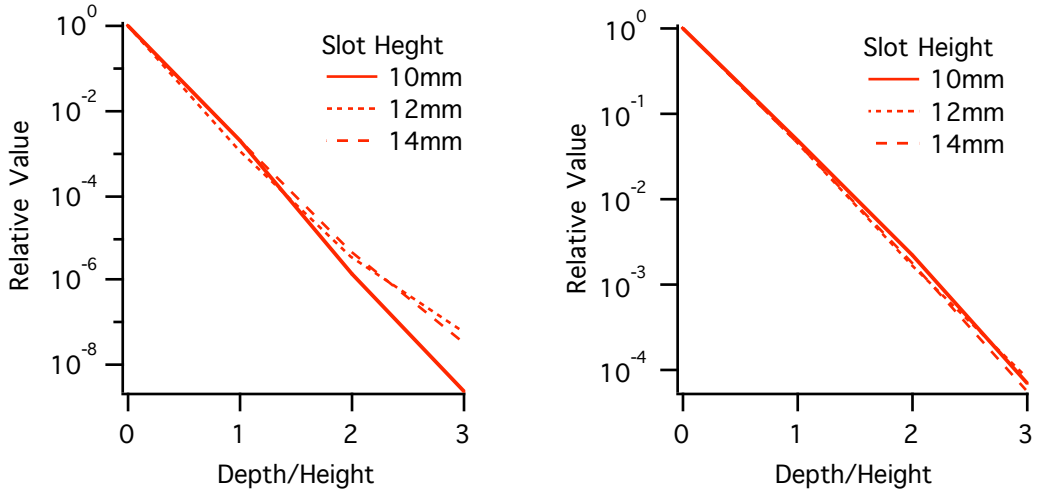

Wake Potential (MAFIA T3) Wall Current (MAFIA S3)

Figure 32. Relative value of the wake functions produced by the element shown in A of Figure 31 and the wall current induced by the charge shown in B of Figure 31.[5]

This result shows that the strength of the wake field and the wall current both exponentially depends only on depth / height, and (Maximum of Wake Functions) $\propto$ (Wall Current)^2 .

IIX. VALIDITY OF TWO-DIMENSIONAL APPROXIMATION

The difference of two-dimensional and three-dimensional models are studied with MAFIA T3. The shapes used is shown in Figure 33. The longitudinal wake functions for the bunch length σ_z=10mm are shown in Figure34 . This shows that the two-dimensional approximation is a good approximation.

The transverse wake functions are shown in Figure 35. The transverse position of the driving charge and the axis for integration are same; for W_{1x}' and W_{1y}', (x,y)=(10mm,0) and (0,10mm), respectively. The d value obtained with equation (18) is 35 mm for x-direction and 20mm for y-direction. Those are the radii of x-direction and y-direction of the ellipse.

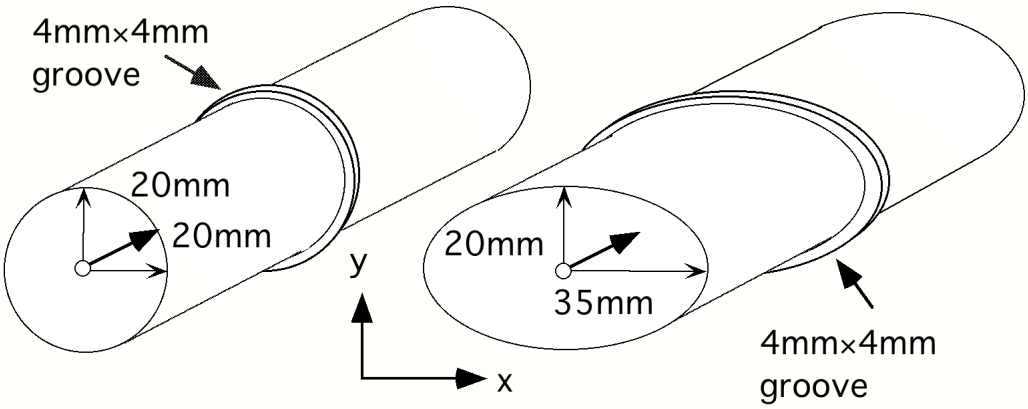

two-dimensional shape three-dimensional shape (real shape)

Figure 33. shapes for the comparison of two-dimensional and three-dimensional simulation.

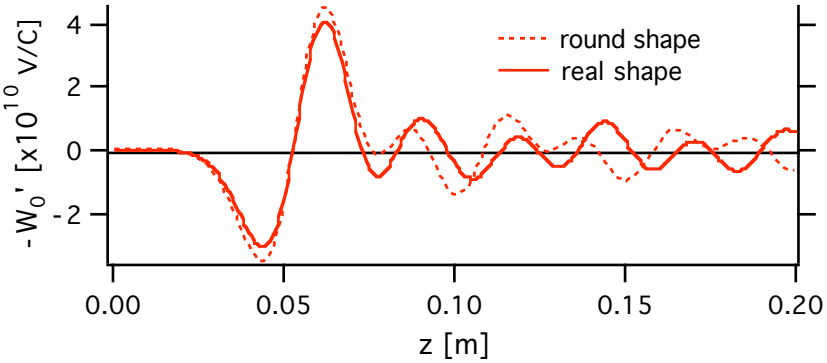

Figure 34. Longitudinal wake functions for the two-dimensional and three-dimensional shapes shown in Figure 33. The bunch length is σ_z=10mm and the bunch center is at z=0.05m.

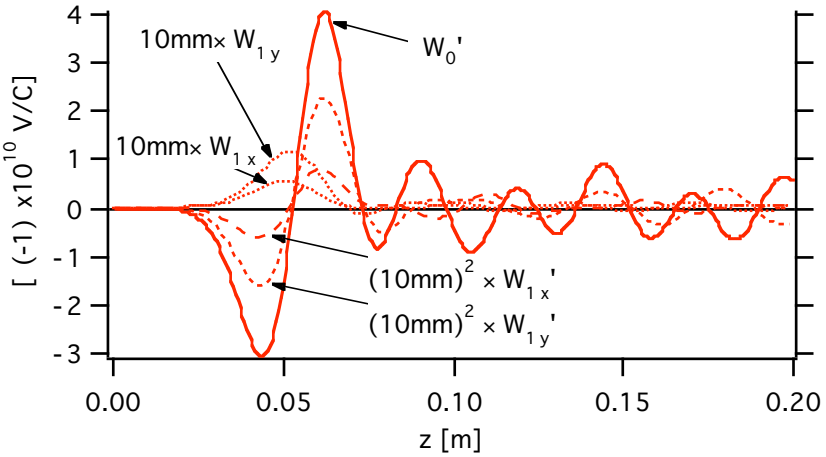

Figure 35. Longitudinal and transverse wake functions
for the three-dimensional shape shown in Figure 33.
The bunch length is σ_z=10mm and the bunch center is at z=0.05m

IX. CONCLUSION

The impedance of the SPring-8 is estimated. The equation (12) is valid with adequate d values.

REFERENCE

[1] For example, R. Klatt and T. Weiland, "Wake Field Calculations with Three-Dimensional BCI," Proc. of Linear Accelerator Conference, SLAC, (1986) 282.

[2] K. L. F. Bane, "Bunch Lengthening in The SLC Damping Rings," SLAC-PUB-5177(1990)

[3] S. Heifets, "Broad Band Impedance of The B-Factory," SLAC/AP-93(1992).

[4] M. Takao, T. Higo and K. L. F. Bane, "Estimation of the Longitudinal Impedance of the ATF Damping Ring," Conference Record of the 1991 IEEE Particle Accelerator Conference, Vol. 2, pp.506-508.

[5] T. Nakamura, "Estimation of Broad Band Impedance of the SPring-8 Storage Ring," Conference Record of the 1993 IEEE Particle Accelerator Conference, Vol.5, pp.3464-3466.

[6] W. Watanabe, et al. ,"Vacuum Chamber and Crotch Absorber for the SPring-8 Storage Ring Vacuum Chamber," Conference Record of the 1993 IEEE Particle Accelerator Conference, Vol.5, pp.3845-3847.
[7] For Example, A. W. Chao, "Physics of Collective Beam Instabilities in High Energy Accelerators," 1993, John-Wiley & Sons Inc. The definintion of z in this paper is minus of z in this book[7].